Self-Phase Modulation in Semiconductor Optical Amplifiers: Impact of Amplified Spontaneous Emission

Prashant P. Baveja, Drew N. Maywar, *Member, IEEE,* Aaron M. Kaplan, and Govind P. Agrawal, *Fellow, IEEE*

***Abstract*—This paper presents a detailed theoretical and experimental study of the impact of amplified spontaneous emission (ASE) on self-phase modulation in semiconductor optical amplifiers (SOAs). A theoretical model of pulse propagation in SOAs is developed that includes the ASE power and its effect on gain-saturation and gain-recovery. We study the impact of ASE on the nonlinear phase shift, frequency chirp, spectrum, and shape of amplified picosecond pulses at a range of drive currents. We verify our predictions experimentally by launching gain-switched picosecond pulses with 3-mW peak power into a commercial SOA exhibiting 9-ps gain-recovery time at a current of 500 mA. Understanding the impact of ASE on SOAs is important for applications that employs SOAs for all-optical signal processing and as data-network amplifiers.**

***Index Terms*—Amplified spontaneous emission (ASE), gain recovery, optical signal processing, self-phase modulation (SPM), semiconductor optical amplifier (SOA), spectral broadening.**

I. Introduction

In FUTURE high-speed telecommunication systems, all-optical signal processing techniques promise to play a prominent role in avoiding electro-optic conversions that may create data-flow bottlenecks. Semiconductor optical amplifiers (SOAs) have been widely used to perform a variety of all-optical functions such as wavelength conversion [1], signal regeneration [2], and pulse reshaping [3]. Compared to their fiber-based counterparts [4]–[6], SOA-based all-optical signal processing techniques have advantages in terms of low-power consumption, a small footprint, and monolithic integration [7]. However, such techniques generally also have one serious limitation. While the Kerr-based nonlinear response of an optical fiber is almost instantaneous [8], the nonlinear response time of a SOA is tied to its carrier lifetime [9] that governs how quickly the SOA gain recovers is typically longer than 0.1 ns [10].

Numerous techniques have been used in the literature to reduce the gain-recovery time of SOAs [11]–[20]. These techniques can be grouped into three categories. The first category involves the use of SOAs made with semiconductor quantum dots [11], [12] or doped quantum wells [13]. The second category involves using a continuous-wave (CW) beam that saturates the SOA because its wavelength lies within the SOA gain spectrum or near the transparency point [14]–[16]. The third category employs the amplified spontaneous emission (ASE) within the SOA to saturate its gain and to reduce its gain-recovery time [17]–[20]. Such SOAs are available commercially with a gain-recovery time as short as 10 ps. They are designed carefully so that they can be driven at high-drive currents (up to 500 mA in our case), and high-ASE and short gain-recovery times are realized only at these high-operating currents [21]. Although the nonlinear effects have been investigated in SOAs employing a holding beam for faster gain recovery [22]–[24], no study has yet addressed the nonlinear effects in SOAs whose gain recovery is sped up by the ASE.

In this paper, we address self-phase modulation (SPM), a fundamental nonlinear effect that leads to spectral broadening of optical pulses. This phenomenon in SOAs was first studied in 1989 [9]. The physical mechanism behind SPM in SOAs was found to be gain saturation, which leads to intensity-dependent changes in the refractive index in response to variations in carrier density. In that work, however, the gain-recovery time, limited by the carrier lifetime, was taken to be much longer than typical pulse widths employed in the experiment [9].

We perform a comprehensive investigation of the impact of ASE-induced gain saturation on signal amplification in SOAs, with emphasis on the SPM phenomenon in the pulsed case. In Section II, we extend the theoretical framework of [9] to include the impact of ASE and derive a simple expression for the SOA amplification factor in the CW case. In Section III, we present CW experimental results and use them to extract a critical device parameter that governs the ASE level at a given current. In Section IV, we use this parameter to show how

Manuscript received December 16, 2009; revised March 26, 2010; accepted April 14, 2010. Date of current version July 23, 2010. This work was supported in part by the National Science Foundation (NSF), under Award ECCS-0822451. The support of NSF does not constitute an endorsement of the views expressed in this article. This paper was recommended by Associate Editor A. A. Hardy.

P. P. Baveja and G. P. Agrawal are with the Institute of Optics, University of Rochester, Rochester, NY 14627 USA (e-mail: baveja@optics.rochester.edu; gpa@optics.rochester.edu).

D. N. Maywar is with the Department of Electrical, Computer, and Telecommunications Engineering Technology, Rochester Institute of Technology, Rochester, NY 14623-5603 USA (e-mail: dnmiee@rit.edu).

A. M. Kaplan is with the University of St Andrews, Fife KY16 9AJ, U.K. (e-mail: akap06@gmail.com).

Color versions of one or more of the figures in this paper are available online at http://ieeexplore.ieee.org.

Digital Object Identifier 10.1109/JQE.2010.2048743

gain-recovery time is reduced at high-drive currents. In Section V, we consider the amplification of picosecond pulses and study the impact of ASE on the SPM-induced nonlinear-phase shift and the corresponding frequency chirp imposed on the pulse. We study theoretically in Section VI the impact of ASE on the shape and spectrum of amplified pulses. In Section VII, we present experimental results on pulse amplification and compare them with theory. The main results of this paper are summarized in Section VIII.

II. Theoretical Model With ASE Effects

When an optical signal is launched into the SOA, its amplitude and phase change because of the gain provided by SOA and the associated changes in the refractive index. To describe this amplification process, we adopt the model developed in [9] and write the signal's electric field in the form

$$\mathbf{E}(\mathbf{r}, t) = Re[\hat{x}F(x, y)A(z, t)e^{i(\beta_0 z-\omega_0 t)}] \tag{1}$$

where $\hat{x}$ is the polarization unit vector, $F(x, y)$ is the transverse optical mode distribution, $A(z, t)$ is the complex amplitude, ω_0 is angular carrier frequency, and $\beta_0 = \bar{n}\omega_0/c$ is the propagation constant of the optical mode with the effective index $\bar{n}$, and c is the speed of light in vacuum.

As discussed in [9], the signal amplitude evolves inside the SOA as

$$\frac{\partial A}{\partial z} + \frac{1}{v_g}\frac{\partial A}{\partial t} = \frac{g}{2}(1 - i\alpha)A \tag{2}$$

where v_g is the group velocity, g is the SOA gain, and α is the linewidth enhancement factor responsible for changes in the mode index with changes in the carrier density that satisfies a rate equation of the form [10]

$$\frac{\partial N}{\partial t} = \frac{I}{qV} - \frac{N}{\tau_c} - \frac{g(N)}{\hbar\omega_0}|A|^2 \tag{3}$$

where V is the active volume and τ_c is the carrier lifetime. The injection of current into an SOA creates electrons and holes, whose density N provides optical gain as $g(z, t) = \Gamma a(N-N_0)$, where Γ is the mode confinement factor, a is the material parameter (referred to as the gain cross-section), and N_0 is the value of carrier density at which the SOA becomes transparent. The carrier density rate equation (3) can be used to obtain the following equation for the optical gain $g(z, t)$ [9]:

$$\frac{\partial g}{\partial t} = \frac{g_0 - g}{\tau_c} - \frac{g|A|^2}{E_{\text{sat}}} \tag{4}$$

where $E_{\text{sat}} = \hbar\omega_0\sigma/a$ is the saturation energy, σ is the mode cross-section, and the unsaturated gain g_0 depends on the injected current I as

$$g_0(I) = \Gamma a N_0(I/I_0 - 1) \tag{5}$$

where $I_0 = qVN_0/\tau_{c0}$ is the current required for transparency and τ_{c0} is the carrier lifetime at $N = N_0$.

In modern SOAs designed for ultrafast gain-recovery, ASE becomes large enough at high-injection currents that it can itself saturate the SOA gain, and the preceding set of equations should be adapted to incorporate the effects of ASE. A general theory of pulse propagation should consider the amplification of spontaneous emission in both the forward and backward directions over the entire SOA gain bandwidth. Because of the stochastic nature of ASE, such a theory is quite complicated. Here, we adopt a simple approach by ignoring the random nature of the amplified signal and treat $A(z, t)$ as the average signal amplitude. However, we take into account the ASE induced gain-saturation by replacing $|A|^2$ in (4) with $|A|^2+P_{\text{ASE}}$, where $P_{\text{ASE}} = P_f + P_b$ represents the sum of ASE powers in the forward and backward directions. The resulting modified gain equation can be written as

$$\frac{\partial g}{\partial t} = \frac{g_0 - g}{\tau_c} - \frac{g(|A|^2 + P_{\text{ASE}})}{E_{\text{sat}}}. \tag{6}$$

Even though P_f and P_b change considerably along the SOA length because of exponential amplification of spontaneous emission, their sum is relatively constant. We simplify the following analysis by treating P_{ASE} as a constant whose value depends only on the current I injected into the SOA.

Before considering amplification of optical pulses, we first focus on the CW case and assume that a CW signal with input power P_{in} is injected into the SOA. Using $A(z) = \sqrt{P}e^{i\phi}$ in (2), the CW signal power, P, and phase, ϕ satisfy

$$\frac{dP}{dz} = g(z)P, \qquad \frac{d\phi}{dz} = -\frac{\alpha}{2}g(z). \tag{7}$$

Setting the time derivative to zero in (6), the signal power $P(z)$ is found to depend on P_{ASE} as

$$\frac{dP}{dz} = \frac{g_0(I)P}{1 + (P + P_{\text{ASE}})/P_{\text{sat}}} \tag{8}$$

where the saturation power P_{sat} is defined as [9]

$$P_{\text{sat}} = \frac{E_{\text{sat}}}{\tau_c} = \frac{\hbar\omega_0\sigma}{a\tau_c}. \tag{9}$$

In the small-signal regime, SOA gain is saturated only by P_{ASE}. Equation (8) can then be integrated easily to obtain $G(I) = P_{\text{out}}/P_{\text{in}}$, where $P_{\text{out}} = P(L)$ and L is the SOA length. The final result is given by

$$G(I) = \exp\left(\frac{g_0(I)L}{1 + P_{\text{ASE}}/P_{\text{sat}}}\right) \tag{10}$$

where both $P_{\text{ASE}}(N)$ and $P_{\text{sat}}(N)$ also depend on I because the carrier density N changes with I.

III. ASE-Induced Gain Saturation

Fig. 1(a) shows the experimental setup used for measuring the small-signal gain of a weak CW signal as a function of drive current using a commercial SOA (by CIP Photonics, Suffolk, U.K.). Table I shows the manufacturer's specifications of this SOA used when it amplifies a 1550-nm signal at a 500-mA drive current. We launched a 1594.4-nm signal with 2-μW power to ensure that it does not saturate the amplifier. The power of amplified signal was measured after passing it through a 1-nm-bandwidth optical bandpass filter (OBPF) to reject the out-of-band portion of the ASE.

The symbols in Fig. 1(b) show the measured values of $\log G$ as a function of drive current I. The coupling and other losses

TABLE I
OPTICAL SPECIFICATIONS OF THE SOA AT 500 MA

Parameter	Value
Small-signal gain	25 dB
Saturated output power	12.5 dBm
Wavelength of gain peak	1570 nm
Saturated gain recovery time ($1/e$)	10 ps
3-dB bandwidth of gain spectrum	35 nm

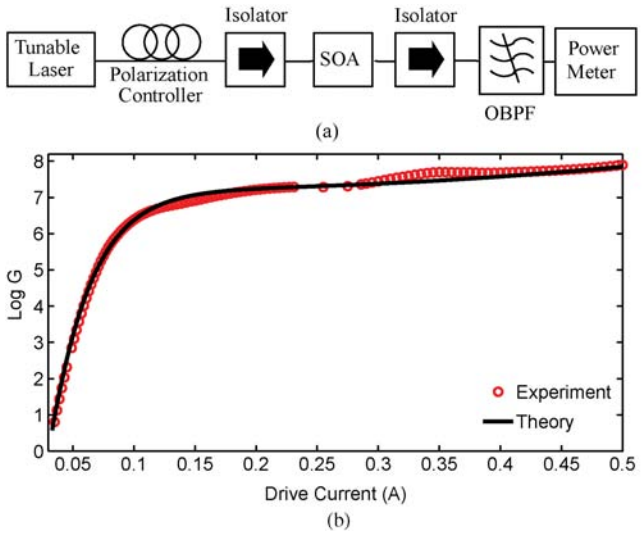

Fig. 1. (a) Experimental setup and (b) measured values of log G as a function of drive current. The solid line corresponds to the best estimate of D from the experimental data (circles).

are included by adding 2 dB to the fiber-to-fiber gain values measured in the experiment. It is evident from this figure that the CW signal is amplified exponentially (or linearly on the semilog plot) for currents of up to about 100 mA, but this exponential growth is reduced dramatically at higher currents. This behavior is because of gain saturation induced by the increasing ASE.

To fit the experimental data, we first consider the low-current regime. We set the time derivative to zero in (3), neglect the last term, and find N at a given value of I by solving

$$\frac{I}{qV} = \frac{N}{\tau_c} \tag{11}$$

where the carrier lifetime, τ_c, itself depends on N. If we include both the radiative and nonradiative recombination processes, this dependence takes the form

$$\frac{1}{\tau_c} = A_{nr} + B_{sp}N + C_a N^2 \tag{12}$$

where A_{nr} is the intrinsic nonradiative recombination rate, B_{sp} is the spontaneous recombination coefficient, and C_a is the Auger recombination coefficient. Combining (11) and (12), the carrier density N, at a drive current I, is a real positive root of a cubic polynomial.

The dimensionless constant $\Gamma a N_0 L$ and transparency current I_0 in (5) are uniquely determined from the experimental data by using the gain values at low-drive currents, at which ASE can be neglected. They are found to be to be 7 and 30 mA, respectively. We know $L = 1$ mm for our device. Using the assumed parameter values from Table II, we deduce the values listed in Table III.

TABLE II
ASSUMED PARAMETER VALUES FOR THE SOA

Parameter	Our Value	Typical Values
Γ	0.4	0.3–0.7
a (m^2)	10.5×10^{-20}	$2.5–4.5\times10^{-20}$
A_{nr} (s^{-1})	3.9×10^{9}	$0.1–4.5\times10^{9}$
B_{sp} (m^3/s)	8.5×10^{-16}	$1–9\times10^{-16}$
C_a (m^6/s)	3.3×10^{-40}	$1–97\times10^{-40}$

TABLE III
DEDUCED PARAMETER VALUES FOR THE SOA

Parameter	Description	Deduced Value
N_o (m^{-3})	Transparency carrier density	1.64×10^{23}
V (m^3)	Active volume	2.83×10^{-16}
σ (m^2)	Mode cross-section	7.07×10^{-13}
$E_{\rm sat}$ (pJ)	Saturation energy	0.824

We now consider the ASE-saturated regime in Fig. 1(b) and note that the ASE power also depends on the carrier density N. Since electron–hole recombination is the source of ASE, we expect ASE to scale as N^2, where both electron and hole densities are proportional to N [10] and assume

$$P_{\rm ASE} = DN^2 \tag{13}$$

where D is a constant of proportionality. The procedure outlined above allows us to calculate $P_{\rm ASE}(N)$ and $P_{\rm sat}(N)$, and consequently $G(I)$, at any drive current. The value of D is estimated by using it as a fitting parameter for the experimental data shown in Fig. 1(b). Its value was found to be 2.32×10^{-50} m^6W. Table II shows the values of parameters used for curve fitting together with typical values employed in the literature for different SOAs [10], [17], [19], [20], [24]–[29]. As seen there, the value of a is larger for our SOA, resulting in a smaller value of N_0 at the same optical gain.

IV. ASE-INDUCED GAIN RECOVERY

We next use our model to study how the gain-recovery time is shortened at high-drive currents by the increasing ASE. Although pump-probe measurements are often performed to measure gain-recovery time, here our objective is to deduce it from the CW data in Fig. 1. For this purpose, we rewrite (6) as

$$\frac{\partial g}{\partial t} = \frac{g_0}{\tau_c} - \frac{g}{\tau_{\rm eff}} - \frac{g|A|^2}{E_{\rm sat}} \tag{14}$$

where the effective gain-recovery time is defined as

$$\frac{1}{\tau_{\rm eff}} = \frac{1}{\tau_c} + \frac{1}{\tau_{\rm ASE}} \tag{15}$$

and we have introduced a new ASE-related recombination time as

$$\frac{1}{\tau_{\rm ASE}} = \frac{P_{\rm ASE}}{E_{\rm sat}} = \frac{DN^2}{E_{\rm sat}} = D_{sp}N^2. \tag{16}$$

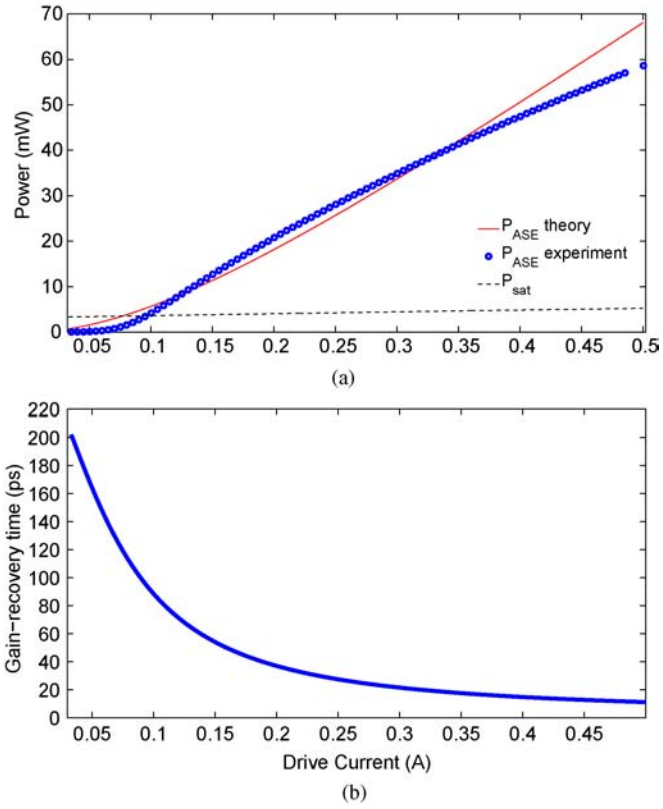

Fig. 2. Calculated values of (a) $P_{\rm ASE}$ and $P_{\rm sat}$, and (b) $\tau_{\rm eff}$ as a function of drive current for the SOA used to obtain the data in Fig. 1. Experimental measurements of $P_{\rm ASE}$ are shown as circles.

Using (12), (15), and (16), $\tau_{\rm eff}$ can be written in the form

$$\frac{1}{\tau_{\rm eff}} = A_{nr} + B_{sp}N + (C_a + D_{sp})N^2. \tag{17}$$

This relation shows that the ASE contribution has the same functional dependence on N as the Auger contribution and can be included in practice by increasing the value of the Auger parameter C_a. Using the calculated value of $E_{\rm sat}$, D_{sp} is found to be 2.75×10^{-38} m^6/s. If we compare this to the value of C_a in Table I, we find that the ASE contribution to $\tau_{\rm eff}$ for our SOA exceeds the Auger contribution by a factor of 83. Clearly, the presence of ASE shortens the gain-recovery time drastically.

Fig. 2(a) shows the calculated values of $P_{\rm ASE}$ and $P_{\rm sat}$ as a function of drive current together with the experimental measurements of $P_{\rm ASE}$ on the same SOA used for Fig. 1. For $I < 70$ mA, $P_{\rm ASE} < P_{\rm sat}$, which justifies our assumption that ASE effects are small at low-drive currents. The experimental measurements of $P_{\rm ASE}$ were carried out by recording the ASE spectrum with an optical spectrum analyzer at various drive currents. The ASE spectrum had a 20-dB bandwidth of over 50 nm and its peak shifted toward shorter wavelengths with increasing drive currents. The power data in Fig. 2(a) was obtained from spectral data by integrating over the entire bandwidth and assuming constant coupling and insertion losses. Because of a wide ASE spectrum and wavelength dependence of losses associated with some of our components, our power data has an uncertainty of about 10% when converted to internal ASE power. With this in mind, the agreement with the model is reasonable at drive currents of up to 400 mA. Larger deviations at higher currents are due the saturation of ASE itself as the SOA gain is saturated, a second-order effect not included in our model.

Fig. 2(b) shows the calculated values of $\tau_{\rm eff}$ as a function of drive current. At low-drive currents, the ASE contribution is negligible, and our SOA has a gain-recovery time near 200 ps ($\tau_{\rm eff} = \tau_c$). As current increases, ASE builds up, as shown in Fig. 2(a), and it leads to a monotonic decrease in the value of $\tau_{\rm eff}$, resulting in a value of about 10 ps at $I = 0.5$ A. This behavior is in agreement with previous studies on these kinds of SOAs [13], [19] and also agrees with the quoted value of 9 ps at $I = 0.5$ A for our SOA.

V. Impact of ASE on SPM-Induced Nonlinear Phase Shift

SPM or its variant, cross-phase modulation, is employed for many all-optical signal processing applications including wavelength conversion [1], signal regeneration [2], pulse compression [30], channel multiplexing/demultiplexing [31], [32], and bit-level logic [33]. The nonlinear phase shift and the resulting chirp imposed on the pulse become important for such SOA-based applications.

In this section, we study the impact of ASE on the SPM-induced nonlinear phase shift imposed on an optical pulse as it propagates through the SOA. In the case of pulses, it is useful to rewrite the amplitude equation (2) in a frame moving with the pulse. Introducing the reduced time as $\tau = t - z/v_g$ together with $A = \sqrt{P}e^{i\phi}$ in (2), the signal power $P(z, \tau)$ and the phase $\phi(z, \tau)$ are found to satisfy [9]

$$\frac{\partial P}{\partial z} = g(z, \tau)P, \qquad \frac{\partial \phi}{\partial z} = -\frac{\alpha}{2}g(z, \tau). \tag{18}$$

These equations look similar to their CW part in (7) except that all variables depend on the time τ implicitly. They can be integrated over the SOA length L to obtain

$$P_{\rm out}(\tau) = P_{\rm in}(\tau)\exp[h(\tau)], \qquad \phi_{nl}(\tau) = -\frac{\alpha}{2}h(\tau) \tag{19}$$

where $h(\tau) = \ln G(\tau) = \int_0^L g(z, \tau)dz$ represents the integrated gain at time τ, $P_{\rm in}(\tau)$ represents the power profile of the input pulse, $P_{\rm out}(\tau)$ represents the power profile of the output pulse, and the SPM-induced nonlinear phase shift is defined as $\phi_{nl}(\tau) = \phi(L, \tau) - \phi(0, \tau)$. We can obtain an equation for $h(\tau)$ by integrating the gain equation (14) over the SOA length [9]. The result is given by

$$\frac{dh}{d\tau} = \frac{g_0 L}{\tau_c} - \frac{h}{\tau_{\rm eff}} - \frac{P_{in}(\tau)}{E_{\rm sat}}(e^h - 1). \tag{20}$$

Once this equation is integrated numerically, both the power and phase profiles of the amplified pulse can be obtained.

The frequency chirp $\Delta\nu_0$ imposed on the pulse is related to the nonlinear phase as $2\pi\Delta\nu_0 = -d\phi_{nl}/d\tau$ [9]. Using $\phi_{nl}(\tau)$ from (19), the chirp is given by

$$\Delta\nu_0(\tau) = \frac{\alpha}{4\pi}\frac{dh}{d\tau} \tag{21}$$

where $dh/d\tau$ is obtained from (20).

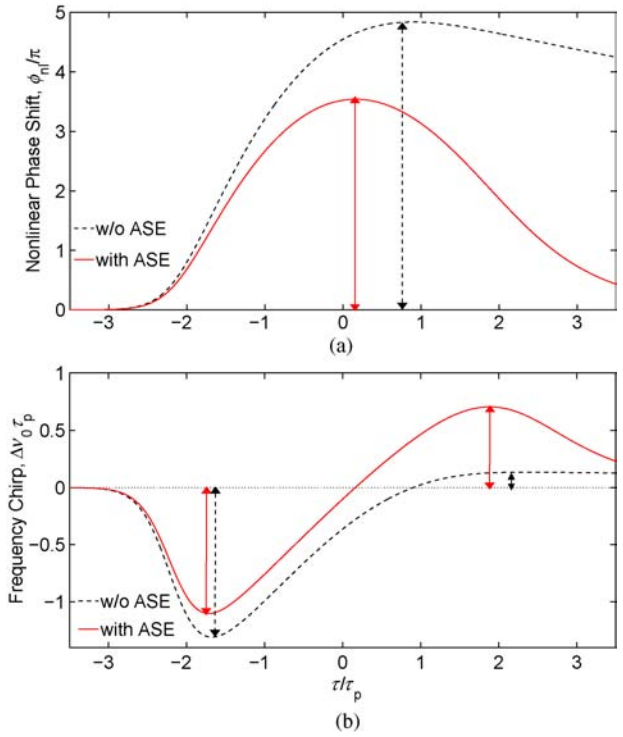

Fig. 3. (a) Nonlinear phase shift and (b) frequency chirp induced on a 20-ps-wide Gaussian pulse by a SOA with large ASE. Dashed lines show the case for which ASE is negligible. The double arrows indicate the maximum value of nonlinear phase shift and red and blue chirp for both the cases.

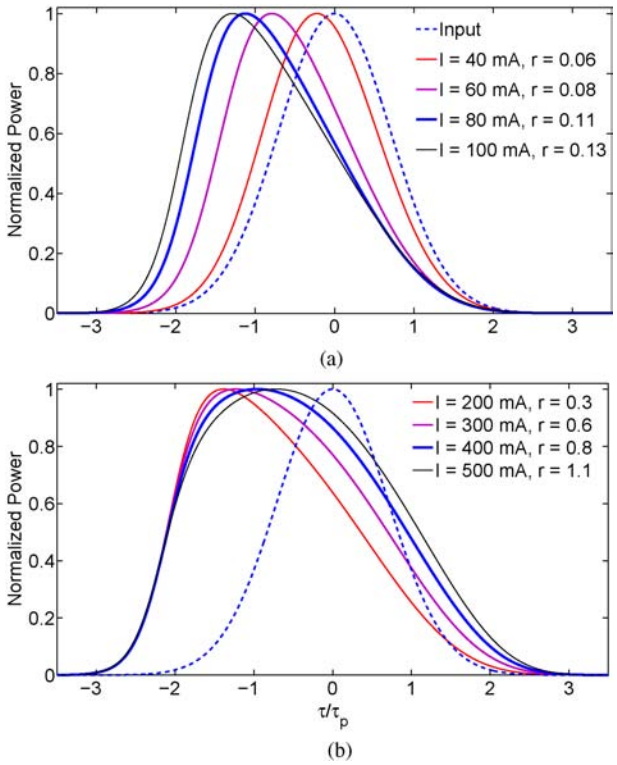

Fig. 4. Output pulse shapes at (a) low-drive currents ($r \leq 0.13$) and (b) high-drive currents ($0.3 < r < 1.1$).

To illustrate the impact of ASE on the nonlinear phase and the frequency chirp, we consider a 20-ps full-width half maximum (FWHM) Gaussian input pulse with the power profile $P(t) = P_0 \exp(-t^2/\tau_p^2)$. When the FWHM is 20 ps, the parameter $\tau_p \approx 12$ ps. We assume that the input pulse energy corresponds to $E_{in}/E_{\text{sat}} = 0.3$. The linewidth enhancement factor α is taken to be 5. The SOA is operated at $I = 0.5$ A at which the small-signal CW amplification factor corresponds to $G = e^{7.8} = 33.9$ dB in Fig. 1. The solid curves in Fig. 3 show the temporal profiles for the nonlinear phase shift $\phi_{nl}(\tau)$ and for the chirp $\Delta\nu_0(\tau)$ using $\tau_{\text{eff}} = 10$ ps, the value we deduced in Section III. For comparison, the dashed lines show the case of a SOA with negligible ASE by using $\tau_{\text{eff}} = \tau_c = 200$ ps. Clearly, ASE affects the SPM process considerably, both qualitatively and quantitatively.

When the ASE effects are negligible, our theory reduces to that of ref [9] because the pulse width is a small fraction of the gain-recovery time of 200 ps. The nonlinear phase shows a rapid increase as the leading edge of the pulse saturates the SOA gain, and a reduction in the carrier density increases the mode index. Since the gain cannot recover much over the pulse duration, the nonlinear phase saturates with only slight reduction in the trailing part of the pulse. The situation changes considerably when ASE reduces the gain-recovery time to 10 ps. Now, the saturated gain can recover within the pulse duration. As a result, the carrier density begins to increase in the trailing region of the pulse. The resulting decrease in the mode index then leads to a rapid decrease of the pulse phase as well. The net result is that the phase profile becomes much more symmetric and begins to mimic the shape of the amplified pulse. This is precisely what occurs in the case of optical fibers whose nonlinearity responds on a femtosecond time scale [8]. The fiber-like features of SPM in SOAs are potentially attractive for designing SOA-based devices such as all-optical regenerators and switches. The nonlinear phase shifts can also be used in an interferometric configuration for ultrafast all-optical signal-processing applications [34].

The chirp profiles in Fig. 3(b) show how ASE-induced changes in the gain-dynamics affect the frequency chirp imposed by the SPM on an amplifying pulse. In the absence of ASE, the pulse experiences a red shift over its leading edge but a negligible blue chirp is imposed on its trailing edge. In the presence of ASE, the extent of red chirp is reduced slightly but there is a significant increase in blue chirp due to ASE-induced faster gain recovery. The net result is an almost linear chirp across the center part of the pulse, a behavior similar to that occurring in optical fibers [8]. This linear chirp is very attractive for compressing the amplified pulse [35]. It is worth noting that the required peak power of pulses is smaller by a factor of 1000 or more when SOAs are compared with optical fibers.

VI. Pulse Shapes and Spectra

Changes induced by ASE in the frequency chirp also affect the spectrum of the amplified pulse. In this section, we look at the shape and the spectrum of the output pulse when a 20-ps Gaussian input pulse is amplified by the SOA at different drive currents. Since the gain-recovery time τ_{eff} is reduced with

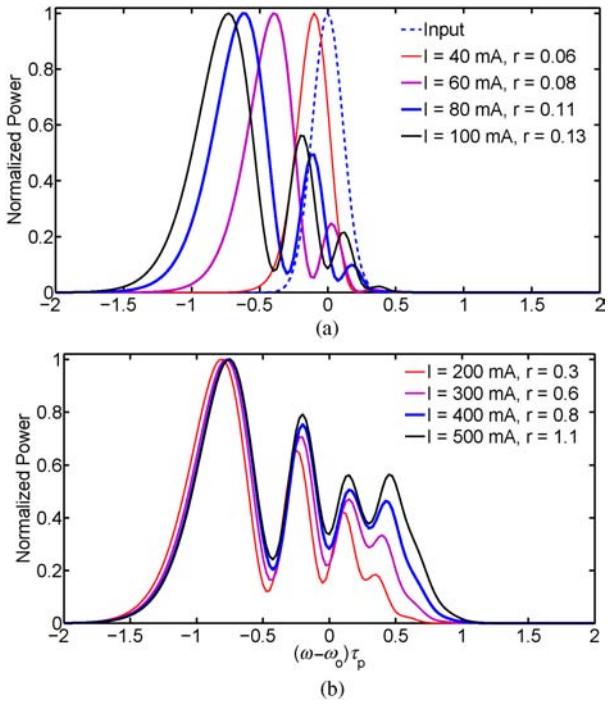

Fig. 5. Output pulse spectrum (a) at relatively low-drive currents ($r \leq 0.13$) and (b) at high currents ($0.3 < r < 1.1$).

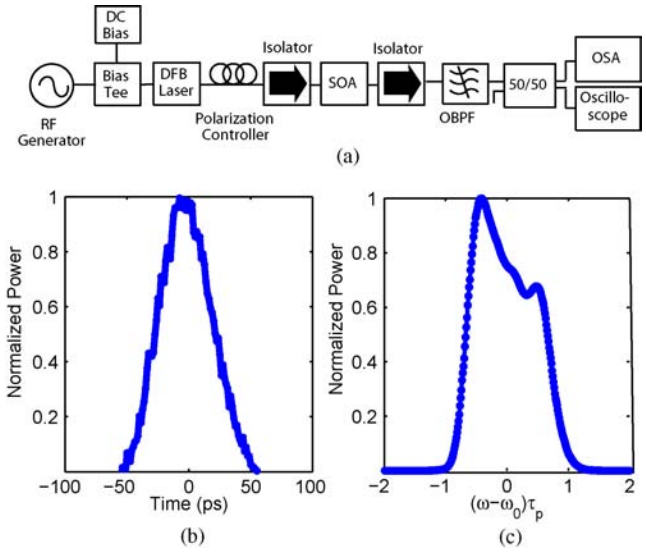

Fig. 6. (a) Experimental setup. (b) Pulse shape and (c) pulse spectrum produced by the gain-switched DFB laser.

increasing currents, we introduce a dimensionless parameter r as the ratio $r = \tau_p/\tau_{\text{eff}}$. For a constant input pulse width, r increases with increasing drive current.

The output pulse shape is obtained from (19), and the corresponding results for different values of r (or I) are shown in Fig. 4. All other parameters are identical to those used in Section IV. At low-drive currents below 100 mA (or $r \leq 0.13$), ASE power is negligible, and the gain-recovery time is much longer than the pulse width, a situation similar to that studied in [9]. As shown in Fig. 4(a), the amplified pulse acquires an asymmetric shape with a leading edge sharper than the trailing edge. This occurs because the leading edge of the pulse experiences full gain, but gain is reduced substantially near the trailing edge, because pulse's leading part saturates the SOA gain. However, at drive currents in the range 200–500 mA corresponding to $0.3 < r < 1.1$, the increasing ASE power begins to saturate the gain and reduce the gain-recovery time, making it comparable to the pulse width at currents near 500 mA. As seen in Fig. 4(b), the pulse becomes more symmetric as drive current increases, with no visible changes near the leading edge of the pulse. Physically, the gain begins to recover so quickly that the training edge begins to experience as much gain as the leading edge of the pulse.

The pulse spectrum is obtained by taking the Fourier transform of the output field $A(L, \tau)$, and the results are shown in Fig. 5 for drive currents ranging from 40 mA to 500 mA and corresponding to $0.06 < r < 1.1$. At low-drive currents of up to 100 mA ($r < 0.13$), output spectrum is highly asymmetric with most of pulse energy contained in a red-shifted spectral lobe. This kind of spectrum is associated with SOAs whose gain-recovery time is much longer compared to the pulse width [9]. At high-drive currents seen in Fig. 5(b) with r in the range 0.3–1.1, energy is transferred from the red to blue side of the pulse spectrum, and the blue-shifted spectral lobes increase in amplitude progressively. These changes in the pulse spectra can be understood in terms of a faster gain recovery induced by increasing ASE. At low-drive currents ($r < 0.1$), the trailing part of the pulse does not experience much blue chirp (see Fig. 3), resulting in an asymmetric red-shifted pulse spectrum. At drive currents of 200 mA or more, ASE power becomes large enough that the gain-recovery time is reduced considerably. This enhanced gain recovery imposes a blue chirp on the trailing part of the pulse and increases spectral symmetry in the output spectrum. This situation is similar to that occurring for optical fibers in which SPM is due to a quasi-instantaneous Kerr-type nonlinearity [8]. For $r > 1$, increase in spectral symmetry is accompanied by a saturation of spectral broadening [36].

VII. Experimental Pulse Spectra

To verify the theory developed in this paper, we have measured pulse spectra for the same SOA whose measured gain under CW conditions is shown in Fig. 1. The experimental setup of Fig. 6(a) was employed for this purpose. We use gain switching [37] of a distributed feedback (DFB) laser to produce optical pulses at a wavelength of 1594.41 nm. The threshold current of the laser was 25 mA at 25 °C. To obtain gain-switched pulses, the laser was biased at 14.9 mA and driven with a 1-GHz radio frequency signal with 64.4 mA peak amplitude. Fig. 6 shows (b) the shape and (c) the spectrum of the resulting gain-switched pulses. The central frequency of 188.23 THz was found using the first moment of the spectrum. The shape of 57-ps pulses was nearly Gaussian with $\tau_p = 34.2$ ps, and their peak power was close to 3 mW. Gain-switched pulses were also chirped with $C = -4.91$ in the notation of [8]. An OBPF with a 3-dB bandwidth of 1 nm was used to reject the out-of-band portion of ASE noise. A 50/50 splitter sends amplified pulses simultaneously

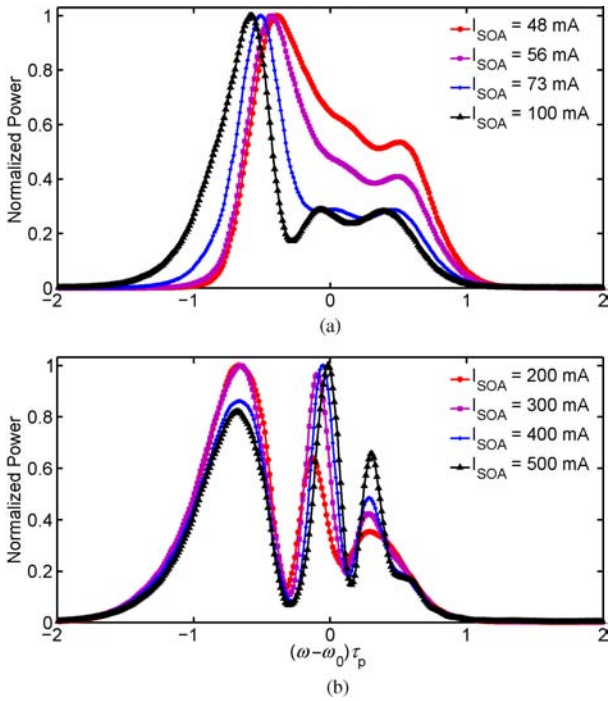

Fig. 7. Observed spectra of amplified pulses at drive current (a) up to 100 mA and (b) beyond 100 mA.

to an optical spectrum analyzer (resolution 0.01 nm) and to a 70-GHz sampling oscilloscope (resolution 1.25 ps).

Fig. 7 shows optical spectra of amplified pulses measured as the drive current is varied from 40 mA to 500 mA. At drive currents up to 100 mA, the spectrum shifts toward the red side with increasing energy in the red lobe. However, a dramatically different behavior occurs for currents beyond 100 mA, as shown in Fig. 7(b), with a dominant central lobe and increasing energy in a blue-shifted spectral lobe. As a result of these changes, the output spectrum progressively becomes more symmetric. These experimental observations are consistent with the theoretical results given in Fig. 5 and confirm that the ASE-induced reduction in the gain-recovery time is responsible for the observed changes at high-drive currents.

VIII. Discussions and Conclusion

This paper has studied, both theoretically and experimentally, the impact of ASE on SPM in SOAs. We used the CW gain measurements and a detailed theoretical model to deduce how ASE shortens the effective gain-recovery time of our SOA to near 10 ps. Our model assumed that the total ASE power is constant along the length of the amplifier and increases with the current injected into the SOA. A numerical model [38] incorporating changes with current in counter propagating ASE spectral components is certainly more accurate than our semi-analytical model. A more quantitative comparison is not possible because our work focuses on modeling recovery speed as function of drive current. We incorporated the current dependence of τ_{eff} and the SOA gain into our simple model and studied the impact of ASE on the amplification of picosecond pulses inside SOAs. Our results show that a shorter gain-recovery time affects the amplification process in several ways. The SPM-induced nonlinear phase shift becomes more symmetric and, consequently, frequency chirp becomes much more linear across the pulse. These features are attractive for designing SOA-based all-optical signal-processing devices such as wavelength converters, regenerators, and switches.

We calculated the shape and spectrum of amplified pulses over a range of drive currents to study how they change with shortening of the gain-recovery time. The pulse shape becomes much more symmetric at high-drive currents because a reduction in the value of τ_{eff} causes the gain to recover fast enough that both the leading and trailing edge of the pulse experience nearly the same dynamic gain profile. For the same reason, the output spectrum becomes more symmetric and resembles that obtained in the case in optical fibers where SPM occurs due to a nearly instantaneous Kerr nonlinearity. We verified our theoretical predictions with an experiment in which we measured pulse spectra using gain-switched input pulses. Our experimental results agree well with the theoretical predictions. The main point to note is that the ASE-induced gain saturation changes the gain dynamics in such a way that the SPM features in SOAs begin to resemble those found in optical fibers, but they occur at peak-power levels that are orders of magnitude lower than those required for optical fibers.

References

[1] J. Leuthold, R. Ryf, D. N. Maywar, S. Cabot, J. Jacques, and S. S. Patel, "Nonblocking all-optical cross-connect based on regenerative all-optical wavelength converter in a transparent demonstration over 42 nodes and 16 800 km," *J. Light. Technol.*, vol. 21, no. 1, pp. 2863–2870, Nov. 2003.

[2] C. Politi, D. Klonidis, and M. J. O'Mahony, "Dynamic behavior of wavelength converters based on FWM in SOAs," *IEEE J. Quantum Electron.*, vol. 42, no. 2, pp. 108–125, Feb. 2006.

[3] G. Contestabile, M. Presi R. Proiletti, and E. Ciaramella, "Optical reshaping of 40-Gb/s NRZ and RZ signals without wavelength conversion," *IEEE Photon. Technol. Lett.*, vol. 20, no. 15, pp. 1133–1135, Jul. 2008.

[4] P. V. Mamyshev, "All-optical regeneration based on self-phase modulation effect," in *Proc. ECOC*, Madrid, Spain, Sep. 20–24, 1998, pp. 475–476.

[5] E. Ciaramella and S. Trillo, "All-optical signal reshaping via four-wave mixing in optical fibers," *IEEE Photon. Technol. Lett.*, vol. 12, no. 7, pp. 849–851, Jul. 2000.

[6] A. Bogoni, P. Ghelfi, M. Scaffardi, and L. Poti, "All-optical regeneration and demultiplexing for 160-Gb/s transmission systems using a NOLM-based three-stage scheme," *IEEE J. Sel. Top. Quantum Electron.*, vol. 10, no. 1, pp. 192–196, Jan. 2004.

[7] T. Houbavlis, K. E. Zoiros, M. Kalyvas, G. Theophilopoulos, C. Bintjas, K. Yiannopoulos, N. Pleros, K. Vlachos, H. Avramopoulos, L. Schares, L. Occhi, G. Guekos, J. R. Taylor, S. Hansmann, and W. Miller, "All optical signal processing and applications within the Esprit project DO_ALL," *IEEE J. Light. Technol.*, vol. 23, no. 2, pp. 781–801, Feb. 2005.

[8] G. P. Agrawal, *Nonlinear Fiber Optics*, 4th ed. Boston, MA: Academic, 2007.

[9] G. P. Agrawal and N. A. Olsson, "Self phase modulation and spectral broadening of optical pulses in semiconductor laser amplifiers," *IEEE J. Quantum Electron.*, vol. 25, no. 11, pp. 2297–2306, Nov. 1989.

[10] G. P. Agrwal and N. K. Dutta, *Semiconductor Lasers*, 2nd ed. New York: Van Nostrand Rienhold, 1993.

[11] M. Sugawara, N. Hatori, M. Ishida, H. Ebe, Y. Arakawa, T. Akiyama, K. Otsubo, T. Yamamoto, and Y. Nakata, "Recent progress in self-assembled quantum-dot optical devices for optical telecommunication," *J. Phys. D: Appl. Phys.*, vol. 38, no. 13, pp. 2126–2134, Jul. 2005.

[12] A. J. Zilkie, J. Meier, P. W. E. Smith, M. Mojahedi, J. S. Aitchison, P. J. Poole, C. N. Allen, P. Barrios, and D. Poitras, "Femtosecond gain and index dynamics in an InAs/InGaAsP quantum dot amplifier operating at 1.55 μm," *Opt. Exp.*, vol. 14, no. 23, pp. 11453–11459, Nov. 2006.

[13] L. Zhang, I. Kang, A. Bhardwaj, N. Sauer, S. Cabot, J. Jaques, and D. T. Nielson, "Reduced recovery time semiconductor optical amplifiers using p-type-doped multiple quantum wells," *IEEE Photon. Technol. Lett.*, vol. 18, no. 22, pp. 2323–2325, Nov. 2006.

[14] M. A. Dupertuis, J. L. Pleumeekers, T. P. Hessler, P. E. Selbmann, B. Deveaud, B. Dagens, and J. Y. Emery, "Extremely fast high-gain and low-current SOA by optical speed-up at transparency," *IEEE Photon. Technol. Lett.*, vol. 12, no. 11, pp. 1453–1455, Nov. 2000.

[15] J. Pleumeekers, M. Kauer, K. Dreyer, C. Burrus, A. G. Dentai, S. Shunk, J. Leuthold, and C. H. Joyner, "Acceleration of gain recovery in semiconductor optical amplifiers by optical injection near transparency wavelength," *IEEE Photon. Technol. Lett.*, vol. 14, no. 1, pp. 12–14, Jan. 2002.

[16] G. Talli and M. J. Adams, "Gain recovery acceleration in semiconductor optical amplifiers employing a holding beam," *Opt. Commun.*, vol. 245, nos. 1–6, pp. 363–370, Jan. 2005.

[17] F. Girardin, G. Guekos, and A. Houbavlis, "Gain recovery of bulk semiconductor optical amplifiers," *IEEE Photon. Technol. Lett.*, vol. 10, no. 6, pp. 784–786, Jun. 1998.

[18] F. Ginovart and J. C. Simon, "Gain dynamics studies of a semiconductor optical amplifier," *J. Opt. A-Pure Appl. Opt.*, vol. 4, no. 3, pp. 283–287, May 2002.

[19] R. Giller, R. J. Manning, G. Talli, R. P. Webb, and M. J. Adams, "Analysis of the dimensional dependence of semiconductor optical amplifier recovery speeds," *Opt. Exp.*, vol. 15, no. 4, pp. 1773–1782, Feb. 2007.

[20] A. M. de Melo and K. Petermann, "On the amplified emission noise modelling of semiconductor optical amplifiers," *Opt. Commun.*, vol. 281, no. 18, pp. 4598–4605, Sep. 2008.

[21] A. Borghesani, "Semiconductor optical amplifiers for advanced optical applications," in *Proc. 8th ICTON*, Nottingham, U.K., Jun. 18–22, 2006, pp. 119–122.

[22] P. M. Gong, J. T. Hsieh, S. L. Lee, and J. Wu, "Theoretical analysis of wavelength conversion based on four-wave-mixing in light-holding SOAs," *IEEE J. Quantum Electron.*, vol. 40, no. 1, pp. 31–40, Jan. 2004.

[23] R. Inohara, K. Nishimura, M. Tsurusawa, and M. Usami, "Experimental analysis of cross-phase modulation and cross-gain modulation in SOA injecting CW assist light," *IEEE Photon. Technol. Lett.*, vol. 15, no. 9, pp. 1192–1194, Sep. 2003.

[24] H. Wang, J. Wu, and J. Lin, "Spectral characteristics of optical pulse amplification in SOA under assist light injection," *J. Light. Technol.*, vol. 23, no. 9, pp. 2761–2771, Sep. 2005.

[25] S. Bischoff, M. L. Nielsen, and J. Mørk, "Improving the all-optical response of SOAs using a modulated holding signal," *J. Light. Technol.*, vol. 22, no. 5, pp. 1303–1308, May 2004.

[26] P. Morel and A. Sharaiha, "Wideband time-domain transfer matrix model equivalent circuit for short pulse propagation in semiconductor optical amplifiers," *IEEE J. Quantum Electron.*, vol. 45, no. 2, pp. 103–114, Feb. 2009.

[27] G. Giuliani and D. D. Alessandro, "Noise analysis of conventional and gain-clamped semiconductor optical amplifiers," *J. Light. Technol.*, vol. 18, no. 9, pp. 1256–1263, Sep. 2000.

[28] D. A. Reid, A. M. Clarke, X. Yang, R. Maher, R. P. Webb, R. J. Manning, and L. P. Barry, "Characterization of a turbo-switch SOA wavelength converter using spectrographic pulse measurement," *IEEE J. Sel. Topics Quantum Electron.*, vol. 14, no. 3, pp. 841–848, May 2008.

[29] R. G. Castrejon and A. Filios, "Pattern-effect reduction using a cross-gain modulated holding beam in semiconductor optical in-line amplifier," *J. Light. Technol.*, vol. 24, no. 12, pp. 4912–4917, Dec. 2006.

[30] N. A. Olsson, G. P. Agrawal, and K. W. Wecht, "16 Gbit/s, 70 km pulse transmission by simultaneous dispersion and loss compensation with 1.5 um optical amplifiers," *Electron. Lett.*, vol. 25, no. 9, pp. 603–605, Apr. 1989.

[31] J. P. Sokoloff, P. R. Prucnal, I. Glesk, and M. Kane, "A terahertz optical asymmetric demultiplexer (TOAD)," *IEEE Photon. Technol. Lett.*, vol. 5, no. 7, pp. 787–790, Jul. 1993.

[32] C. Schubert, C. Schmidt, S. Ferber, R. Ludwig, and H. G. Weber, "Error-free all-optical add-drop multiplexing at 160 Gbit/s," *Electron. Lett.*, vol. 39, no. 14, pp. 1074–1075, Jul. 2003.

[33] J. Dong, X. Zhang, S. Fu, J. Xu, P. Shum, and D. Huang, "Ultrafast all-optical signal processing based on single semiconductor optical amplifier and optical filtering," *IEEE J. Sel. Topics Quantum Electron.*, vol. 14, no. 3, pp. 770–778, May 2008.

[34] Y. Ueno, S. Nakamura, and K. Tajima, "Nonlinear phase shifts induced by semiconductor optical amplifiers with control pulses at repetition frequencies in the 40-160-GHz range for use in ultrahigh-speed all-optical signal processing," *J. Opt. Soc. Am. B*, vol. 19, no. 11, pp. 2573–2589, Nov. 2002.

[35] G. P. Agrawal, *Applications of Nonlinear Fiber Optics*. Boston, MA: Academic, 2001.

[36] P. P. Baveja, D. N. Maywar, A. M. Kaplan, and G. P. Agrawal, "Spectral broadening in ultrafast semiconductor optical amplifiers induced by gain dynamics and self-phase modulation," *Opt. Lett.*, vol. 35, no. 3, pp. 294–296, Feb. 2010.

[37] K. Y. Lau, "Gain switching of semiconductor injection laser," *Appl. Phys. Lett.*, vol. 52, no. 4, pp. 257–259, Jan. 1988.

[38] X. Li, M. J. Adams, D. Alexandropoulos, and I. F. Lealman, "Gain recovery in semiconductor optical amplifiers," *Opt. Commun.*, vol. 281, no. 13, pp. 3466–3470, Jul. 2008.

Prashant P. Baveja received the B.Eng. degree from the Delhi College of Engineering, University of Delhi, New Delhi, India, in 2006. He is currently working toward the Ph.D. degree in optics from the Institute of Optics, University of Rochester, Rochester, NY.

He was an Undergraduate Researcher at Delhi College of Engineering. His current research interests include nonlinear optics in semiconductor optical amplifiers, all-optical signal processing, nonlinear fiber optics, optical communication, optical networking, and Raman amplification.

Drew N. Maywar (S'97–M'06) received the B.S., M.S., and Ph.D. degrees in optics from the Institute of Optics, University of Rochester, Rochester, NY, in 1993, 1997, and 2000, respectively, and the B.A. degree in religion from the same university in 1993.

In 2000, he was a Technical Staff Member with Bell Laboratories, Murray Hill, NJ, where he co-developed Lucent's LambdaXtreme transmission system. In 2003, he was a Lead Scientist with the Laboratory for Laser Energetics, University of Rochester, where he was responsible for the performance of a nuclear-fusion-enabling 30-kJ, 60-beam ultraviolet laser and oversaw a research program in nonlinear photonics. Since 2009, he has been an Assistant Professor of Telecommunications Engineering Technology with the Department of Electrical, Computer, and Telecommunications Engineering Technology, Rochester Institute of Technology, Rochester, NY. He is the co-author of over 30 journal papers on lightwave-communication systems.

Aaron M. Kaplan received the B.S. degree in optics and the M.S. degree in nonlinear optics and bistability for all-optical signal processing from the University of Rochester, Rochester, NY, in 2006 and 2009, respectively.

In 2006, he joined the Laboratory for Laser Energetics, University of Rochester, as a Lead Engineer for the front-end systems group of the high-power Omega fusion laser system. He is currently with the University of St. Andrews, Fife, U.K.

Govind P. Agrawal (M'83–SM'86–F'96) received the M.S. and Ph.D. degrees from the Indian Institute of Technology Delhi, New Delhi, India, in 1971 and 1974, respectively.

After holding positions with the Ecole Polytechnique, Paris, France, the City University of New York, and AT&T Bell Laboratories, Murray Hill, NJ, he joined the faculty of the Institute of Optics at the University of Rochester, Rochester, NY, in 1989, where he is currently a Professor of Optics and Physics, and also a Senior Scientist with the Laboratory for Laser Energetics. He has published seven books and 350 research papers in the field of lightwave technology.

Dr. Agrawal is a Fellow of the Optical Society of America, and a Life Fellow of the Optical Society of India.